GL03463

GEOPHYSICS, VOL. 38, NO. 4 (AUGUST 1973), P. 719–736, 11 FIGS., 1 TABLE

INTERPRETATION OF DIPOLE-DIPOLE RESISTIVITY SURVEYS USING A HEMISPHEROIDAL MODEL†

H. M. BIBBY* AND G. F. RISK*

The solutions for the potential due to a current source near a hemispheroidal body of finite resistivity, which have been given by Cook and Van Nostrand, are adapted for use with dipole-dipole resistivity arrays. In the limiting case where the current dipole is at a large distance from the hemispheroid a simple expression is obtained for the apparent resistivity measured at the center of the hemispheroid. For an arbitrary placement of current electrodes, apparent resistivities are obtained by summing a double series involving the associated Legendre functions.

Theoretical results using differently shaped hemispheroids are compared with field data obtained from several dipole-dipole resistivity surveys of the hot water reservoir of the Broadlands Geothermal Field, New Zealand. The comparison enables an estimate to be made of the depth of the geothermal reservoir.

INTRODUCTION

During the period 1965–1971, a detailed study of the Broadlands geothermal area (see Figure 1) was made by the New Zealand government to determine the feasibility of generating electrical power from the high-temperature (up to 300°C) high-pressure (up to 2 MPa[1] at the well-head) fluid which is contained in the porous rocks of the geothermal field. The study included geophysical, geologic, and geochemical investigations as well as the drilling of 25 wells to depths ranging from 750 to 2400 m. Some of the factors which determine the economic life of a geothermal power station are the volume of hot water and the volume of hot rock contained in the geothermal reservoir. These can be estimated from the total volume of the reservoir and the porosity of the rocks within it. Although an extensive drilling program is the most reliable way to obtain this information, a reasonable estimate of the total volume of the geothermal reservoir can be obtained much more cheaply by determining the volume of conductive material from resistivity measurements.

The resistivity of a rock in a geothermal environment is controlled by the proportions and resistivities of interstitial materials contained within it. From drilling results it is known that in the vicinity of Broadlands the rocks in the upper 2 km have an average porosity of about 25 percent. In the geothermal reservoir the porewater has a very low resistivity because of its high temperature and its large content of dissolved salts (typically about 0.35 ohm-m at 300°C with a chloride ion content of 1500 mg/l). The rocks also contain appreciable amounts of conductive minerals, chiefly clays and zeolites. Thus, the rocks of the geothermal reservoir have resistivities (2–5 ohm-m) which are 10 to 50 times smaller than the resistivities of rocks in the surrounding country. Hence, the location and the extent of a geothermal reservoir can be determined by suitable ground resistivity methods.

Initial resistivity surveys of the Broadlands geothermal area used methods of shallow penetration. Risk et al (1970) reported the results of two surveys using the Wenner fixed spacing method with electrode spacings of 180 m and 550 m. Attempts to obtain resistivity information at large depths using the Wenner array with greater spac-

[1] In SI units MPa is the symbol for megapascal; 1 MPa = 10^6 N/m^2 = 10 bar.

† Manuscript received by the Editor July 10, 1972; revised manuscript received November 13, 1972.

* Department of Scientific and Industrial Research, Wellington, New Zealand.

© 1973 Society of Exploration Geophysicists. All rights reserved.

UNIVERSITY OF UTAH
RESEARCH INSTITUTE
EARTH SCIENCE LAB.

ings were not very successful because of the difficulty in laying out the great lengths of cable required. Conventional sounding methods, with the Schlumberger or Wenner arrays, were not used because of the impracticability of correcting for the disturbing influences of the boundaries of the geothermal field. Attention was then given to dipole-dipole resistivity methods which have been used elsewhere to measure resistivities to depths as great as 30 km (Anderson and Keller, 1966). To aid interpretation it became necessary to look for a simple model for which theoretical apparent resistivities can be calculated and which has approximately the same shape as the geotherm reservoir.

Results from the Wenner surveys have sho that the Broadlands geothermal reservoir is a proximately circular in plan at the surface, a along most of its perimeter has a nearly vertic boundary down to a depth of at least 500 Hence, a hemispheroid with a vertical axis rotation was chosen as the theoretical model f the geothermal reservoir. Having fixed the cent and the surface radius of the hemispheroid model from the results of the Wenner surveys, t depth to the bottom of the hemispheroid can b

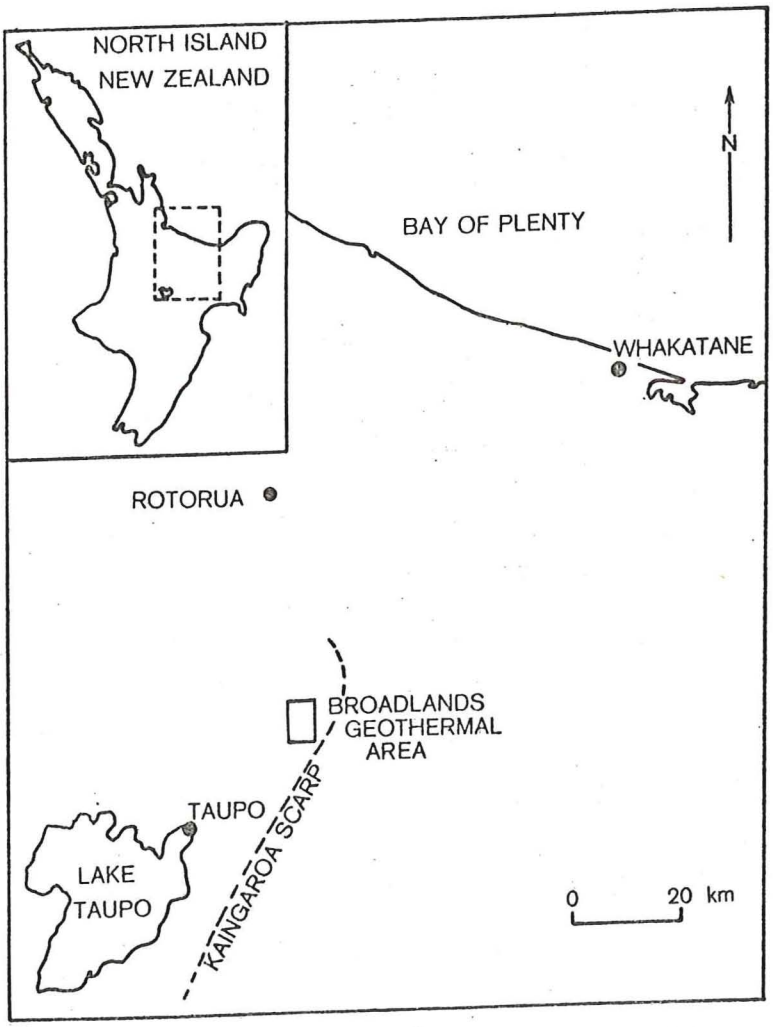

FIG. 1. Location map of Broadlands geothermal area, New Zealand.

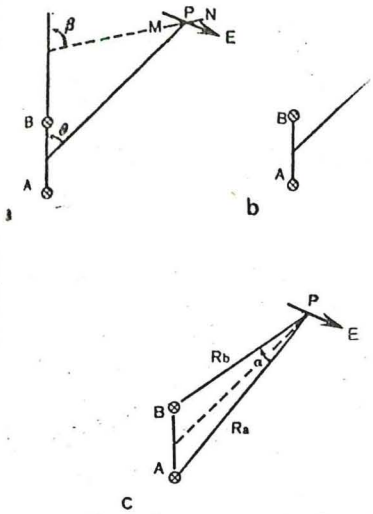

FIG. 2. Electrode arrangements. Curre ween electrodes A and B produces electric at point P. (a) Single receiver dipole iver consisting of two dipoles M_1N_1, oximation for very small receiver dipole

aried so as to obtain the best fit t ipole resistivity observations.

DIPOLE-DIPOLE METHOD OF RESIS MEASUREMENT

A generalized form of the dipole- vity array which is used most commo 966; Keller, 1966; Zohdy, 1970) i igure 2a. A current is passed betwe rodes of the current dipole AB and ntial difference between the electr eceiver dipole MN. For arrays of thi ch (1968) has pointed out that there the angles θ and β for which the a stivities obtained will be strongly in y lateral inhomogeneities which ma particular, since only one compo ctric field strength vector $\mathbf{E}$ is meas ngle receiver dipole used in this me y point there will be a particular or e receiver dipole for which no accur e apparent resistivity can be obtain At Broadlands, two receiver dipole M_2N_2, which were approximately pe re used to measure the potentia used by a current I in the curren e Figure 2b). When the receiver di e small compared with the distance

same shape as the geotherm

ne Wenner surveys have sho
nds geothermal reservoir is a
lar in plan at the surface, a
perimeter has a nearly vertic
o a depth of at least 500
heroid with a vertical axis
en as the theoretical model
servoir. Having fixed the cent
radius of the hemispheroid
sults of the Wenner surveys, t
om of the hemispheroid can b

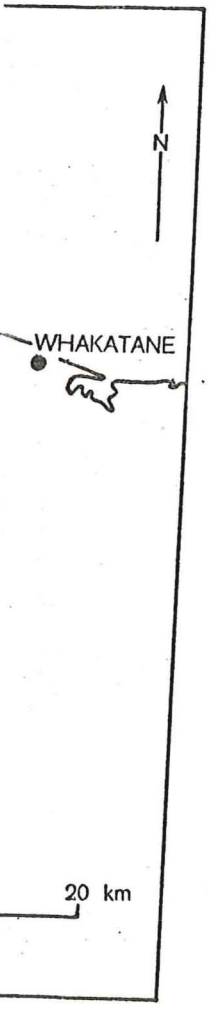

Zealand.

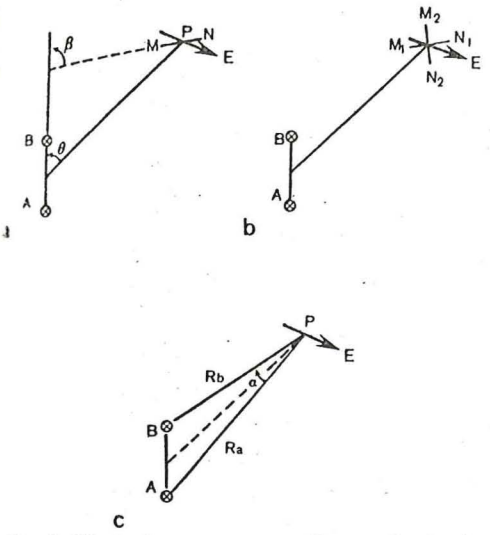

FIG. 2. Electrode arrangements. Current flowing between electrodes A and B produces electric field strength E at point P. (a) Single receiver dipole MN. (b) Receiver consisting of two dipoles M_1N_1, M_2N_2. (c) Approximation for very small receiver dipoles.

varied so as to obtain the best fit to the dipole-dipole resistivity observations.

DIPOLE-DIPOLE METHOD OF RESISTIVITY MEASUREMENT

A generalized form of the dipole-dipole resistivity array which is used most commonly (Al'pin, 1966; Keller, 1966; Zohdy, 1970) is shown in Figure 2a. A current is passed between the electrodes of the current dipole AB and causes a potential difference between the electrodes of the receiver dipole MN. For arrays of this type Fröhlich (1968) has pointed out that there are ranges of the angles θ and β for which the apparent resistivities obtained will be strongly influenced by any lateral inhomogeneities which may be present. In particular, since only one component of the electric field strength vector E is measured by the single receiver dipole used in this method, then at any point there will be a particular orientation of the receiver dipole for which no accurate value of the apparent resistivity can be obtained.

At Broadlands, two receiver dipoles M_1N_1 and M_2N_2, which were approximately perpendicular, were used to measure the potential differences caused by a current I in the current dipole AB (see Figure 2b). When the receiver dipole lengths are small compared with the distance between the current and received dipoles, two components of E are obtained. If the components of E, say E_1 and E_2, are measured at azimuths θ_1 and θ_2, respectively, the magnitude of E is

$$|\mathrm{E}| = [E_1^2 + E_2^2 - 2E_1E_2\cos(\theta_2 - \theta_1)]^{\frac{1}{2}} / |\sin(\theta_2 - \theta_1)|,$$

and its azimuth is

$$\arctan[(E_2\cos\theta_1 - E_1\cos\theta_2) / (E_1\sin\theta_2 - E_2\sin\theta_1)].$$

Definition of apparent resistivity

No convention has been established for defining the apparent resistivity when the quantity measured at the receiver site is the vector E rather than just a single component of it. Although it would be possible to use a modification of the definition of apparent resistivity for a four-electrode array (Keller and Frischknecht, 1966), we have used a different approach.

Following the criterion generally used for defining apparent resistivity, the measurement is assumed to have been made over a hypothetical uniform earth. The apparent resistivity is defined here as the value which the resistivity of the uniform earth must have in order to produce in the receiving array an electric field strength with the same magnitude (but not necessarily the same direction) as the observed electric field strength. Let R_a and R_b be position vectors, of magnitudes R_a and R_b, of the receiver site P relative to the current electrodes A and B, respectively, and α the angle included between them (as shown in Figure 2c). For a uniform half-space of resistivity ρ, and a current I, the electric field strength vector E_{unif} measured at P will be

$$\mathrm{E}_{unif} = \frac{\rho I}{2\pi}[\mathrm{R}_a/R_a^3 - \mathrm{R}_b/R_b^3].$$

The magnitude of this vector $|\mathrm{E}_{unif}|$ is

$$|\mathrm{E}_{unif}| = \frac{\rho I}{2\pi}[R_a^{-4} + R_b^{-4} - 2R_a^{-2}R_b^{-2}\cos\alpha]^{\frac{1}{2}}.$$

Hence, using the definition given above, the apparent resistivity ρ_a at point P is the value which ρ must take in the above equation in order to

make the value of $|E_{unif}|$ calculated at P equal to the value of $|E|$ observed at P. Thus,

$$\rho_a = 2\pi |E| [R_a^{-4} + R_b^{-4} - 2R_a^{-2}R_b^{-2}\cos\alpha]^{-\frac{1}{2}} I^{-1}. \quad (1)$$

The measurement of two components of the electric field eliminates the need for avoiding particular positions as was required for all dipole-dipole arrays measuring only one component. In addition, deviations of the measured direction of the electric field can be used as an indication of the location of discontinuities.

During the Broadlands survey the current dipole was kept in the same location, while the receiver array was moved to occupy a large number of sites over the survey area. Details of the field procedures and instrumentation used at Broadlands have been published by Risk et al (1970).

APPARENT RESISTIVITY NEAR A HEMISPHEROID

Cook and Van Nostrand (1954) have given equations for the potential caused by a current source near a hemispheroidal body of resistivity which contrasts with that of the surrounding material. However, they have presented only a few numerical examples with the Lee and Wenner electrode configurations. Seigel (1952) has computed some theoretical curves using single current electrode arrays for traverses along the axis of rotation of a buried oblate spheroid. This choice of traverse greatly simplified the computations. Apparently, solutions for dipole-dipole arrays have not been computed before, nor has an attempt been made to estimate the depth of a body of hemispheroidal shape.

The model to be examined is illustrated in Figure 3. A hemispheroid of resistivity ρ'' is embedded in a uniform half-space of resistivity ρ'. The surface radius of the hemispheroid is R and its variable depth is D. By adjusting the ratio D/R, a complete range of shapes lying between a shallow disc-like structure ($D \ll R$) and a cylinder ($D \gg R$) can be studied. Figure 4 shows vertical cross-sections of several hemispheroids with different values of D/R.

The electric potential produced by a current electrode which injects a current I into the half-space $z \leq 0$ is given by Cook and Van Nostrand (1954). The potential for a current dipole can be

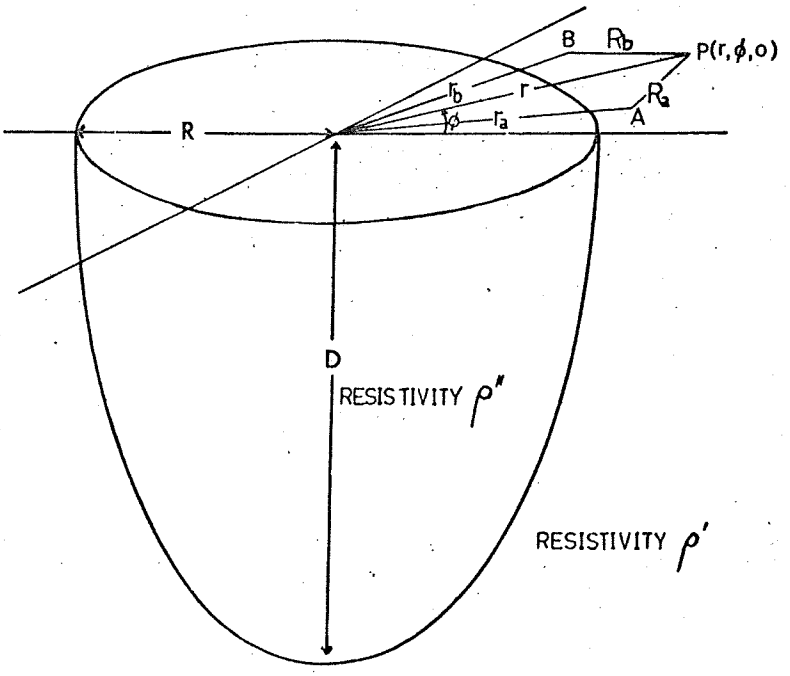

FIG. 3. Hemispheroidal body used in theoretical study showing electrode arrangement.

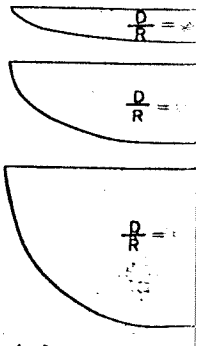

FIG. 4. Vertical cross-sections

found by combining solutions fo
trodes.

Consider two current electrod
ated on the surface $z=0$ at radii r
ϕ_a and ϕ_b, respectively (see Figu
matical expression for the poten
face at point $P(r, \phi, 0)$ takes th
depending on whether the curre
placed both outside, one inside
or both inside the hemispheroid.

For a prolate hemispheroid (D

$$U(r, \phi, 0) = \frac{I\rho'}{2\pi}\left\{\left(\frac{1}{R_a} - \frac{1}{R_b}\right)\right.$$

$$\times \left[\frac{(n-m)!}{(n+m)!} P\right.$$

$$\left. \times \frac{P_n^m(\eta_1)Q_n^m(\eta)}{P_n^m(\eta)Q_n^m(\eta_1)}\right)$$

where

$$\eta = \left[\frac{r^2}{D^2 - R^2} + 1\right]$$

$$\eta_1 = \frac{D}{(D^2 - R^2)^{1/2}},$$

and R_b are the horizontal dista
(z) are associated Legendre fun
and $P_n^{m\prime}(z)$, $Q_n^{m\prime}(z)$ are their de

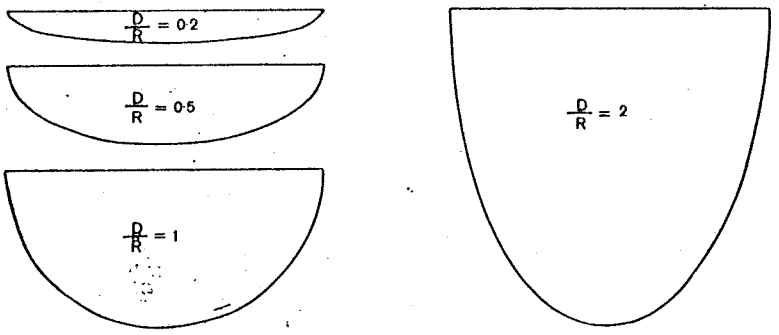

FIG. 4. Vertical cross-sections of hemispheroids with various ratios of depth to surface radius (D/R).

ound by combining solutions for two single electrodes.

Consider two current electrodes A and B, situated on the surface $z=0$ at radii r_a, r_b and azimuths ϕ_a and ϕ_b, respectively (see Figure 3). The mathematical expression for the potential U on the surface at point $P(r, \phi, 0)$ takes three distinct forms depending on whether the current electrodes are placed both outside, one inside and one outside, or both inside the hemispheroid. For each of these cases the expression for the potential also depends on whether P lies inside or outside the hemispheroid. The case of an oblate hemispheroid ($D<R$) is further complicated, requiring distinct forms when P lies either inside or outside a circle of radius $(R^2-D^2)^{\frac{1}{2}}$.

The potential on the surface at point P is given here in the case when both current electrodes lie outside the hemispheroid. The remaining forms of the solution are given in Appendix A.

For a prolate hemispheroid ($D>R$) the potential U is given by

$$U(r,\phi,0)=\frac{I\rho'}{2\pi}\left\{\left(\frac{1}{R_a}-\frac{1}{R_b}\right)+\frac{(\rho''-\rho')}{(D^2-R^2)^{1/2}}\sum_{n=0}^{\infty}\sum_{m=0}^{n}\frac{(2n+1)(2-\delta_{m0})}{(-1)^m}\right.$$
$$\times\left[\frac{(n-m)!}{(n+m)!}P_n^m(0)\right]^2\frac{P_n^{m\prime}(\eta_1)\left[Q_n^m(\eta_a)\cos m(\phi-\phi_a)-Q_n^m(\eta_b)\cos m(\phi-\phi_b)\right]}{\rho' P_n^{m\prime}(\eta_1)Q_n^m(\eta_1)-\rho'' P_n^m(\eta_1)Q_n^{m\prime}(\eta_1)}$$
$$\left.\times\begin{matrix}P_n^m(\eta_1)Q_n^m(\eta)\\P_n^m(\eta)Q_n^m(\eta_1)\end{matrix}\right\}\quad\text{for}\quad\begin{matrix}r>R\\r<R\end{matrix}, \tag{2}$$

where

$$\eta=\left[\frac{r^2}{D^2-R^2}+1\right]^{1/2},\quad \eta_a=\left[\frac{r_a^2}{D^2-R^2}+1\right]^{1/2},\quad \eta_b=\left[\frac{r_b^2}{D^2-R^2}+1\right]^{1/2},$$
$$\eta_1=\frac{D}{(D^2-R^2)^{1/2}},\quad\text{and}\quad\delta_{m0}=\begin{matrix}1, & m=0\\0, & m\neq 0\end{matrix}.$$

R_a and R_b are the horizontal distances from P to the current electrodes A and B, respectively. $P_n^m(z)$, $Q_n^m(z)$ are associated Legendre functions of the first and second kind, degree n, order m (see Appendix B), and $P_n^{m\prime}(z)$, $Q_n^{m\prime}(z)$ are their derivatives with respect to z.

For an oblate hemispheroid ($D<R$) the potential U takes the form

$$U(r,\phi,0)=\frac{I\rho'}{2\pi}\left\{\left(\frac{1}{R_a}-\frac{1}{R_b}\right)+\frac{i(\rho''-\rho')}{(R^2-D^2)^{1/2}}\sum_{n=0}^{\infty}\sum_{m=0}^{n}\frac{(2n+1)(2-\delta_{m0})}{(-1)^m}\right.$$
$$\times\left[\frac{(n-m)!}{(n+m)!}P_n^m(0)\right]^2\frac{P_n^{m\prime}(i\zeta_1)[Q_n^m(i\zeta_a)\cos m(\phi-\phi_a)-Q_n^m(i\zeta_b)\cos m(\phi-\phi_b)]}{\rho' P_n^{m\prime}(i\zeta_1)Q_n^m(i\zeta_1)-\rho'' P_n^m(i\zeta_1)Q_n^{m\prime}(i\zeta_1)}$$
$$\left.\begin{array}{l}P_n^m(i\zeta_1)Q_n^m(i\zeta)\\ \times P_n^m(i\zeta)Q_n^m(i\zeta_1)\\ i^{n+m}P_n^m(\mu)Q_n^m(i\zeta_1)\end{array}\right\}\quad\begin{array}{ll}r>R\\ \text{for}\quad R>r>(R^2-D^2)^{1/2},\\ (R^2-D^2)^{1/2}>r\end{array}\qquad(3)$$

where

$$\zeta=\left[\frac{r^2}{R^2-D^2}-1\right]^{1/2},\quad \zeta_a=\left[\frac{r_a^2}{R^2-D^2}-1\right]^{1/2},\quad \zeta_b=\left[\frac{r_b^2}{R^2-D^2}-1\right]^{1/2},$$
$$\zeta_1=\frac{D}{(R^2-D^2)^{1/2}},\qquad \mu=\left[1-\frac{r^2}{R^2-D^2}\right]^{1/2},\quad\text{and}\quad i=\sqrt{-1}.$$

In the limiting case $D=R$ (the hemisphere) both forms of potential reduce to

$$U(r,\phi,0)=\frac{I\rho'}{2\pi}\left\{\left(\frac{1}{R_a}-\frac{1}{R_b}\right)+\frac{(\rho''-\rho')}{(\rho''+\rho')}\sum_{n=0}^{\infty}\frac{n(\rho''+\rho')R^{n+1}}{[\rho''+n(\rho''+\rho')]}\right.\qquad(4)$$
$$\left.\times\left[P_n^0[\cos(\phi-\phi_a)]r_a^{-n-1}-P_n^0[\cos(\phi-\phi_b)]r_b^{-n-1}\right]\begin{array}{l}R^n/r^{n+1}\\ r^n/R^{n+1}\end{array}\right\}\quad\begin{array}{ll}\text{for}&r>R\\ &r<R\end{array}$$

The electric field can be readily obtained by taking the gradient of the potential. In radial and tangential directions the components E_r and E_ϕ, respectively, are

$$E_r=\frac{-r}{D^2-R^2}\frac{\partial U}{\eta\partial\eta},\qquad E_\phi=-\frac{\partial U}{r\partial\phi}\qquad\text{(prolate case);}\qquad(5)$$
$$E_r=\frac{-r}{D^2-R^2}\frac{\partial U}{i\zeta\partial(i\zeta)},\qquad E_\phi=-\frac{\partial U}{r\partial\phi}\qquad\text{(oblate case).}$$

Thus, from equation (1), the theoretical apparent resistivity is given by:

$$\rho_a=2\pi(E_r^2+E_\phi^2)^{1/2}[R_a^{-4}+R_b^{-4}-2R_a^{-2}R_b^{-2}\cos\alpha]^{-1/2}I^{-1}.\qquad(6$$

COMPUTATION OF APPARENT RESISTIVITIES FOR THE GENERAL CASE

Calculating apparent resistivities for the general case where the two current electrodes are at a finite distance from the center requires the evaluation of E_r and E_ϕ, as defined by equation (5). This, in turn, requires the summation of derivatives of the double series given in equations (2) and (3).

A computer program has been developed to d this using the Elliott 503 electronic computer operated by the Department of Scientific an Industrial Research.

The summation of the double series necessitate the generation of the Legendre functions for bo real and imaginary variables. The simplest mea of generating these functions is by the use of r

currence relations (see, for 1953) between functions of degree. Care must be taken relations, however, as the e will increase with the numbe rence relation has to be used. not be used because the error idly. When these errors were r relations were used for the ge and $Q_n^m(z)/m!$. The inclusion found to reduce the error intr rence process. A summary of given in Appendix B.

The series were summed in of 40 terms and were found vergent for most electrode vergence is slower either whe trodes approach the boundar id, or when the parameter D

ASYMPTOTIC CASE FOR DISTAN

For making a preliminary in

$$\frac{1}{R_a}=\sum_{n=0}^{\infty}\sum_{m=0}^{n}\frac{(2n$$

Substituting in (2), the potent

$$U=\frac{I\rho'\rho''}{2\pi(D^2-R^2)}$$
$$\times\frac{(n+m)!}{(n-m)!}$$

where the Wronskian relation,

$$P_n^m(\eta)Q_n^{m\prime}(\eta)-$$

has been used.

Now consider the special case tance from the hemispheroid. ctions of the second kind can

$$Q_n^m(\eta_a)\simeq(-$$

The series of equation (7) is rap

$$U\simeq\text{Constant}+$$

ence relations (see, for example, Erdélyi, i) between functions of different order and ree. Care must be taken in the use of these tions, however, as the error in the function increase with the number of times the recur- ce relation has to be used. Some relations can- be used because the error increases very rap- . When these errors were negligible, recurrence tions were used for the generation of $P_n^m(z)/m!$ $Q_n^m(z)/m!$. The inclusion of the factor $m!$ was nd to reduce the error introduced by the recur- ce process. A summary of the methods used is en in Appendix B.

The series were summed in n up to a maximum 10 terms and were found to be rapidly con- gent for most electrode placings. The con- gence is slower either when the current elec- des approach the boundary of the hemispher- or when the parameter D/R becomes large.

ASYMPTOTIC CASE FOR DISTANT CURRENT DIPOLE

For making a preliminary interpretation of the field data it is useful to study an asymptotic case in which the expression for the apparent resistivity is reduced to a much simpler form. In general, the apparent resistivity is a function of the position of current electrodes, the position of potential array, the ratio of depth to radius of the hemispheroid (D/R), and the ratio of outer resistivity to inner resistivity, ρ'/ρ''. When the current electrodes are at a large distance from the hemispheroid and the potential array is at the center, a simple expression can be derived for ρ_a which is a function of only D/R and ρ'/ρ''. Hence, the dependence of ρ_a on these two parameters can be studied more easily.

Consider the case when the two current electrodes are outside the hemispheroid. The potential given by equation (2) can be rewritten in an alternative form, using the expansion of the reciprocal distance in the appropriate spheroidal coordinates. For $r<r_a$, in the case of a prolate hemispheroid $(D>R)$, the reciprocal distance is given by

$$\frac{1}{R_a} = \sum_{n=0}^{\infty}\sum_{m=0}^{n} \frac{(2n+1)(2-\delta_{m0})}{(-1)^m(D^2-R^2)^{1/2}}\left[\frac{(n-m)!}{(n+m)!}P_n^m(0)\right]^2 P_n^m(\eta)Q_n^m(\eta_a)\cos m(\phi-\phi_a).$$

bstituting in (2), the potential within the hemispheroid becomes

$$U = \frac{I\rho'\rho''}{2\pi(D^2-R^2)^{1/2}}\sum_{n=0}^{\infty}\sum_{m=0}^{n}(2n+1)(2-\delta_{m0})\left[\frac{(n-m)!}{(n+m)!}P_n^m(0)\right]^2 \times \frac{(n+m)![Q_n^m(\eta_a)\cos m(\phi-\phi_a) - Q_n^m(\eta_b)\cos m(\phi-\phi_b)]}{(n-m)!(\eta_1^2-1)[\rho' P_n^{m\prime}(\eta_1)Q_n^m(\eta_1) - \rho'' P_n^m(\eta_1)Q_n^{m\prime}(\eta_1)]}P_n^m(\eta), \tag{7}$$

ere the Wronskian relation,

$$P_n^m(\eta)Q_n^{m\prime}(\eta) - P_n^{m\prime}(\eta)Q_n^m(\eta) = (-1)^m(n+m)!/(1-\eta^2)(n-m)!,$$

s been used.

Now consider the special case where both r_a, $r_b \gg D(>R)$, that is, the current dipole is at a large stance from the hemispheroid. Under these conditions, η_a and η_b are large, and the associated Legendre actions of the second kind can be approximated by

$$Q_n^m(\eta_a) \simeq (-1)^m(n+m)!n!2^n/(2n+1)!\eta_a^{n+1} + O(\eta_a^{-n-2}).$$

e series of equation (7) is rapidly convergent, and to order $n=1$ is

$$U \simeq \text{Constant} + \frac{I\rho'\rho''}{\pi(\eta_1^2-1)}\frac{[\cos(\phi-\phi_a)/r_a^2 - \cos(\phi-\phi_b)/r_b^2]}{\rho' P_1^{1\prime}(\eta_1)Q_1'(\eta_1) - \rho'' P_1'(\eta_1)Q_1^{1\prime}(\eta_1)}r. \tag{8}$$

Hence, the apparent resistivity within the hemispheroid becomes

$$\rho_a = \frac{2\rho'\rho''}{(\eta_1^2 - 1)\left|\rho' P_1^{1\prime}(\eta_1)Q_1^1(\eta_1) - \rho'' P_1^1(\eta_1)Q_1^{1\prime}(\eta_1)\right|}. \quad (9a)$$

At the center of the hemispheroid the approximations made above are very good because the first-order correction terms ($n=2$) vanish, thus giving a higher-order approximation.

Similarly, the apparent resistivity at the center of an oblate hemispheroid ($D<R$) in the same limiting case reduces to

$$\rho_a = \frac{2\rho'\rho''}{(\zeta_1^2 + 1)\left|\rho' P_1^{1\prime}(i\zeta_1)Q_1^1(i\zeta_1) - \rho'' P_1^1(i\zeta_1)Q_1^{1\prime}(i\zeta_1)\right|}. \quad (9b)$$

Equations (9a) and (9b) can be readily evaluated to give apparent resistivities for this asymptotic case.

USE OF ASYMPTOTIC APPROXIMATION

Apparent resistivities computed from equations (9a) and (9b) for the limiting case where the current electrodes are at a large distance from the hemispheroid and the potential array is at the center are shown in Figures 5a and 5b. The curves show the variation of the dimensionless ratios ρ_a/ρ' and ρ_a/ρ'', respectively, as a function of D/R for different ratios of inner to outer resistivity. In Figure 5b only curves for ρ'/ρ'' greater than unity are shown.

Some useful inferences can be made from these curves.

(1) It can be seen from Figure 5a that a low-resistivity hemispheroid ($\rho'/\rho''>1$) produces a more detectable effect than a high-resistivity hemispheroid ($\rho'/\rho''<1$). In the la for very large resistivity contrasts a of D/R, the apparent resistivity m center approaches a limiting value the resistivity of the material out spheroid. Hence, with distant cur a high-resistivity hemispheroid is ect with dipole-dipole arrays.

(2) A thin localized overburden nted by a hemispheroid with a D/R, and the disturbing effect of su n a dipole-dipole resistivity travers ined. It is evident from Figure gh-resistivity overburden the effe r $D/R<0.1$, but, for a low-re rden, it is still appreciable, in s R as small as 0.01.

(3) For field data obtained wit ectrodes at a large distance from t d, an estimate of D/R can be

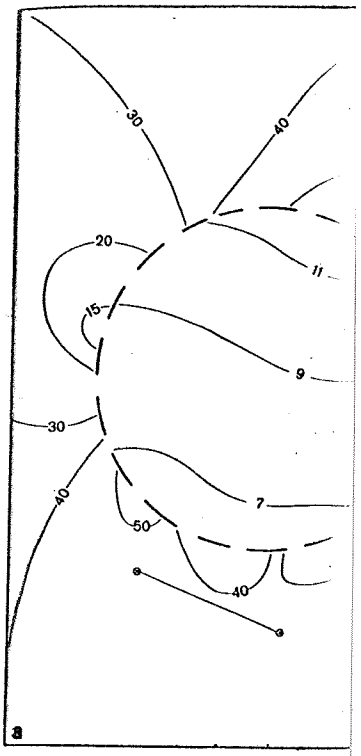

FIG. 6. Comparison of theoretical a show apparent resistivity in ohm-m thermal reservoir as a hemispheroid wi survey at Broadlands.

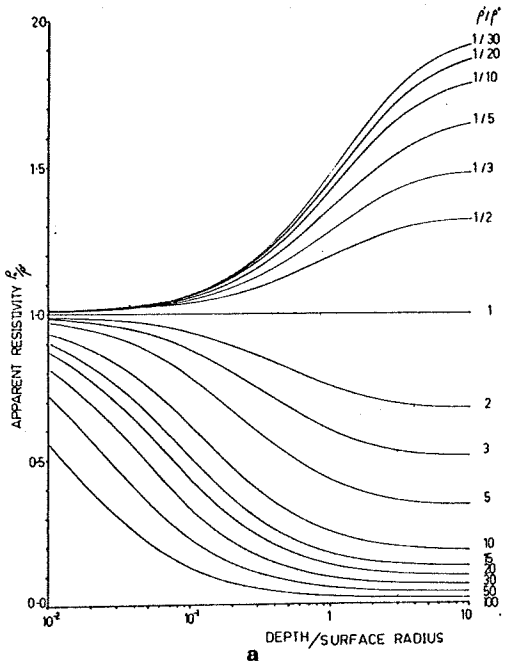

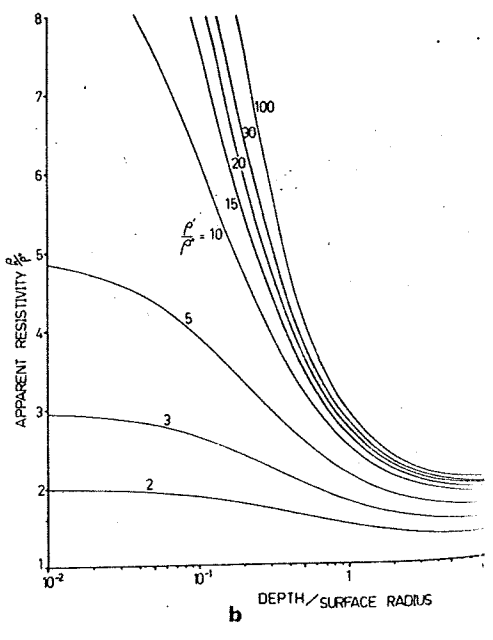

FIG. 5a. Apparent resistivity at the center of a hemispheroidal body for r_a, $r_b \gg R$. ρ_a/ρ' versus D/R for various ratios, $\rho':\rho''$.

FIG. 5b. Apparent resistivity at the center of a hemispheroidal body for r_a, $r_b \gg R$. ρ_a/ρ'' versus D/R for various ratios, $\rho':\rho''$, for $\rho'>\rho''$.

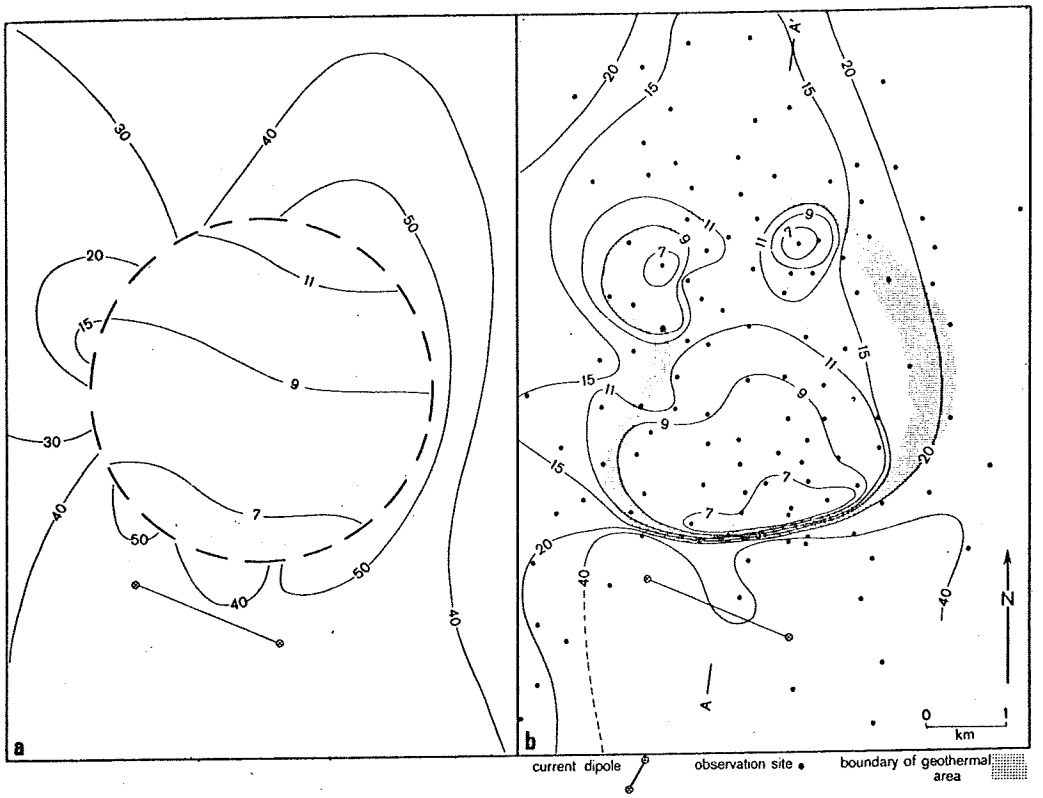

FIG. 6. Comparison of theoretical and observed results with the same current electrode placement. Contours show apparent resistivity in ohm-m measured at the surface. (a) Theoretical representation of Broadlands geothermal reservoir as a hemispheroid with parameters $\rho''=3$ ohm-m, $\rho'=45$ ohm-m, $D/R=0.8$. (b) Results from field survey at Broadlands.

hemispheroid ($\rho'/\rho''<1$). In the latter case, even for very large resistivity contrasts and large values of D/R, the apparent resistivity measured at the center approaches a limiting value of only twice the resistivity of the material outside the hemispheroid. Hence, with distant current electrodes a high-resistivity hemispheroid is difficult to detect with dipole-dipole arrays.

(2) A thin localized overburden can be represented by a hemispheroid with a small value of D/R, and the disturbing effect of such a structure on a dipole-dipole resistivity traverse can be determined. It is evident from Figure 5a that for a high-resistivity overburden the effect is negligible for $D/R<0.1$, but, for a low-resistivity overburden, it is still appreciable, in some cases, for D/R as small as 0.01.

(3) For field data obtained with the current electrodes at a large distance from the hemispheroid, an estimate of D/R can be made from a knowledge of ρ_a, ρ', and ρ''. In addition, it is shown in Figure 5b that for ratios of D/R near unity, and for $\rho'/\rho''>10$, the apparent resistivity is more sensitive to changes in D/R than to changes in ρ'/ρ''. This enables an estimate of D/R to be made without an exact value being known for the outer resistivity.

In the dipole-dipole surveys at Broadlands the current electrodes were never more than a distance of 2 radii from the center of the geothermal reservoir. Hence, they cannot be considered to be a large distance away. Nevertheless, it is of interest to obtain a range of values of D/R from the data available. Estimates of ρ' and ρ'/ρ'' have been made from earlier resistivity measurements using the Wenner array (Risk et al, 1970). They are 2.5 ohm-m $\leq\rho''\leq$3.5 ohm-m, and $10\leq\rho'/\rho''\leq30$. From the dipole-dipole surveys the average value of ρ_a obtained at the center of the geothermal reservoir is 9 ohm-m. This gives $2.5\leq\rho_a/\rho''\leq3.6$.

Therefore, assuming that the geothermal reservoir is hemispheroidal in shape, these limitations constrain its parameters to lie within the shaded area in Figure 5b. The corresponding limits for D/R can be read off and give $0.4 \leq D/R \leq 1.5$. This range is rather large but is useful as a guide for more accurate analysis using the general solution to the problem.

DETERMINATION OF PARAMETERS OF THE BEST-FITTING HEMISPHEROID

Several dipole-dipole resistivity surveys have been made of the Broadlands area, but only three of these are suitable for determining the parameters (D/R, ρ', and ρ'') of the best-fitting hemispheroid. Contour maps of apparent resistivity for these three surveys are shown in Figures 6b, 7b, and 8b, which also show the positions of the current electrodes and the receiver array sites. For each measurement, the apparent resistivity has been plotted at the site of the receiver array. The shaded annulus gives the best estimate of the position of the boundary of the geothermal area as deduced from all the available resistivity information.

The noncircular surface cross-section of the geothermal area makes it difficult to match theoretical and observed data at all the observation points simultaneously. For this reason the matching was made using only those observation points which were inside the geothermal area and lay within 0.5 km of a line through the center of the geothermal area and the center of the current dipole. These sections are indicated by AA', BB', and CC' in Figures 6b, 7b, and 8b, respectively.

For a section across the surface of the hemispheroid, the curves of theoretical apparent resistivity for a current dipole can be fitted accurately to a polynomial of the

$$\rho_a/\rho'' = a_0 + a_1 x + a_2$$

where x is the distance from the spheroid, and the coefficients functions of ρ'/ρ'' and D/R. sentative values of ρ'/ρ'' and in this way, intermediate curv by interpolation. Sufficient acc by neglecting terms in power

A least-squares technique match the survey data with the and hence obtain the values D/R which are listed in Table tempt was made to find the bes all three parameters. Howeve from the results obtained (show of each data set in Table 1) the determined accurately by this

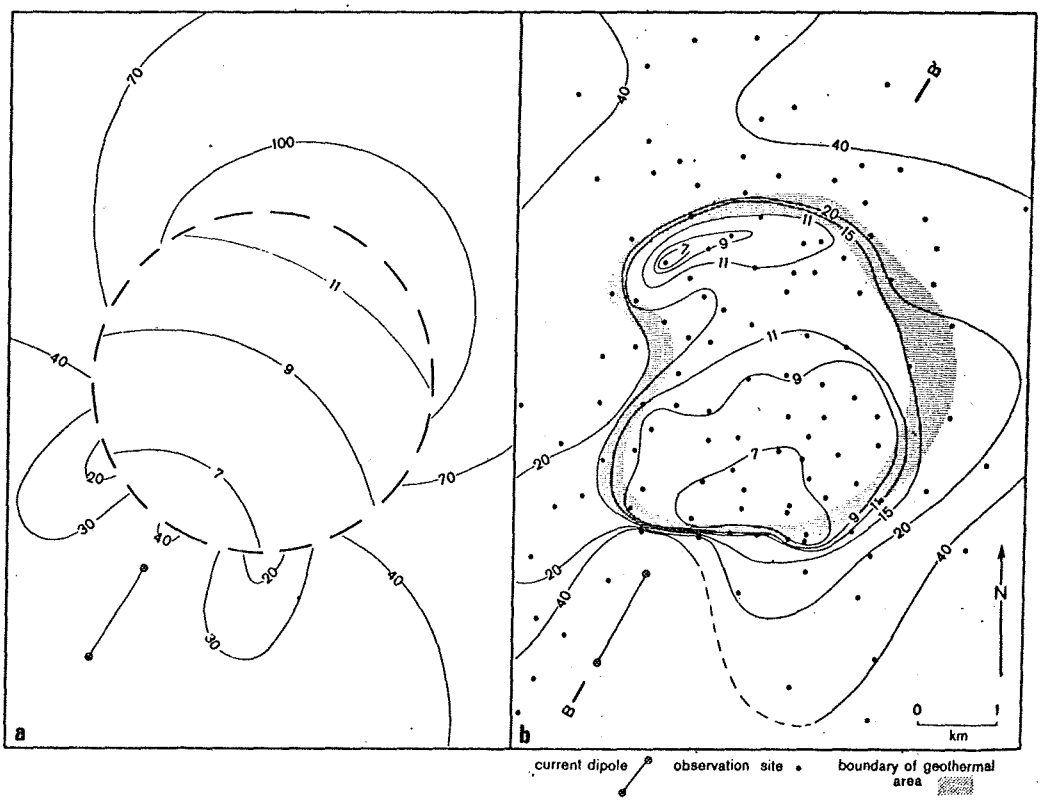

FIG. 7. Comparison of theoretical and observed results with the same current electrode placement. Contours show apparent resistivity in ohm-m measured at the surface. (a) Theoretical representation of Broadlands geothermal reservoir as a hemispheroid with parameters $\rho''=3$ ohm-m, $\rho'=36$ ohm-m, $D/R=0.8$. (b) Results from field survey at Broadlands.

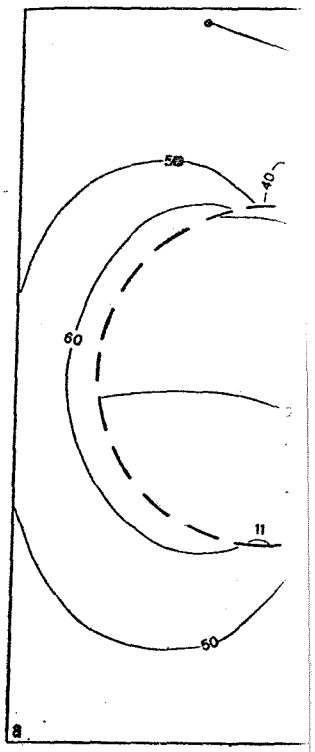

FIG. 8. Comparison of theoret
show apparent resistivity in ohm
thermal reservoir as a hemispher
field survey at Broadlands.

rement, the apparent resistivity
at the site of the receiver array.
ius gives the best estimate of the
oundary of the geothermal area as
ll the available resistivity in-

r surface cross-section of the geo-
kes it difficult to match theoreti-
data at all the observation points
or this reason the matching was
those observation points which
othermal area and lay within 0.5
igh the center of the geothermal
ter of the current dipole. These
cated by AA', BB', and CC' in
d 8b, respectively.
across the surface of the hemi-
ves of theoretical apparent re-
rrent dipole can be fitted ac-

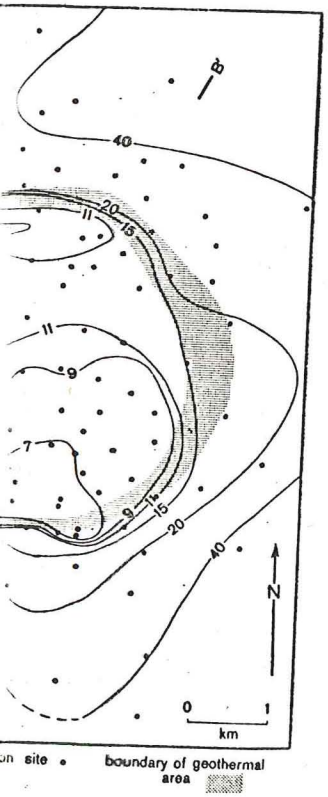

t electrode placement. Contours
presentation of Broadlands geo-
-m, D/R=0.8. (b) Results from

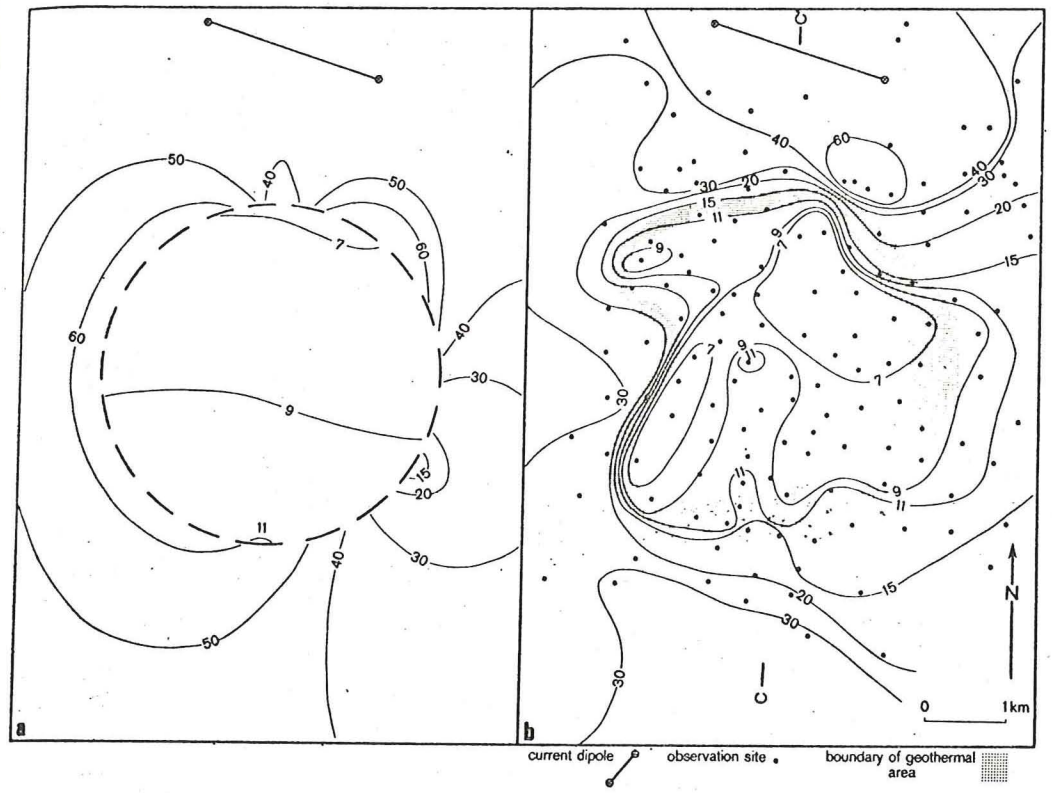

FIG. 8. Comparison of theoretical and observed results with the same current electrode placement. Contours show apparent resistivity in ohm-m measured at the surface. (a) Theoretical representation of Broadlands geothermal reservoir as a hemispheroid with parameters ($\rho''=3$ ohm-m, $\rho'=45$ ohm-m, $D/R=0.8$. (b) Results from field survey at Broadlands.

curately to a polynomial of the form

$$\rho_a/\rho'' = a_0 + a_1 x + a_2 x^2 + \cdots, \quad (10)$$

where χ is the distance from the edge of the hemispheroid, and the coefficients a_0, a_1, a_2, $\cdots$ are functions of ρ'/ρ'' and D/R. Curves for representative values of ρ'/ρ'' and D/R were obtained in this way, intermediate curves being obtainable by interpolation. Sufficient accuracy was obtained by neglecting terms in power greater than x^2.

A least-squares technique was then used to match the survey data with the theoretical curves and hence obtain the values for ρ'', ρ'/ρ'', and D/R which are listed in Table 1. Initially an attempt was made to find the best-fitting values for all three parameters. However, it can be seen from the results obtained (shown in the first line of each data set in Table 1) that ρ'/ρ'' cannot be determined accurately by this method. Consequently, further fittings were made for particular values of ρ'/ρ''. The different estimates of ρ'' and D/R are reasonably consistent, but the standard error in D/R is greater than had been hoped for. Examples of the fitting are illustrated in Figures 9 and 10, which correspond to profiles along section BB' (Figure 7b) and CC' (Figure 8b), respectively.

The best overall estimate for D/R is $D/R=0.96 \pm 0.32$, where the bounds have been determined from the mean of the variances of the estimates obtained from the three surveys (see Table 1). Taking the mean radius of the geothermal area as 2.1 km, a depth of 2.0 km is obtained, and the corresponding volume of the hemispheroid is 19 km^3.

COMPARISON OF OBSERVED AND THEORETICAL RESISTIVITIES

Figures 6a, 7a, and 8a show contour maps of the theoretical apparent resistivities obtained from

Table 1. Values obtained for the parameters ρ'', D/R, and ρ'/ρ'' by a least-squares fitting of field and theoretical data along traverse lines through the center of the geothermal area and the current electrodes.

	Values obtained by fitting			Values set
	ρ'' (ohm-m)	D/R	ρ'/ρ''	ρ'/ρ''
First Survey, Figure 6	3.4 ± 0.3	0.98 ± 0.23	44 ± 30	--
	3.0 ± 1.0	0.75 ± 0.41	--	15
	3.0 ± 0.9	0.81 ± 0.38	--	20
	3.0 ± 0.9	0.86 ± 0.41	--	30
Second Survey, Figure 7	3.4 ± 0.8	0.99 ± 0.30	16 ± 27	--
	3.4 ± 0.4	0.96 ± 0.20	--	15
	3.3 ± 0.4	1.02 ± 0.21	--	20
	3.3 ± 0.3	1.05 ± 0.24	--	30
Third Survey, Figure 8	2.9 ± 0.5	0.91 ± 0.40	35 ± 40	--
	2.8 ± 1.1	0.72 ± 0.55	--	15
	2.9 ± 0.9	0.82 ± 0.50	--	20
	2.9 ± 0.6	0.93 ± 0.45	--	30

equation (6) for a hemispheroid of surface area equal to the average area enclosed by the annulus shown in Figures 6b, 7b, and 8b. The values chosen for the parameters D/R, ρ', and ρ'' are given in the captions of the figures. Since the calculations were made for current electrodes in the same relative positions as were used in the field surveys, a direct comparison of observed and theoretical results is possible.

In addition to making estimates of D/R, an important use of the theoretical results is to provide a criterion for determining which apparent resistivity variations are caused by the presence of a hemispheroid and which are caused by other features.

It can be seen in Figures 6, 7, and 8 that there is reasonable agreement between the theoretical and observed resistivities. Inside the geothermal area quite good agreement is found, although there are several areas where significant differences occur. At the boundary where the theoretical apparent resistivities have a discontinuity, the observed resistivities increase sharply along most of the perimeter, but along the eastern side a gradual change in resistivity is observed rather than a discontinuity. Although the shape of the boundary is nearly circular, a significant irregularity occurs in the northeast. Outside the boundary, the agreement is poor, but in some areas where either high- or low-apparent resistivities have been predicted, similar highs or lows are observed.

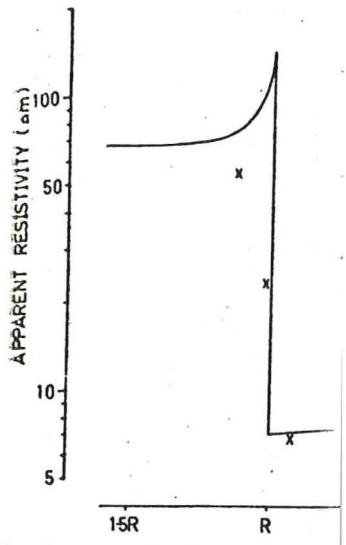

Fig. 9. Curve of theoretical apparen... center of the current dipole. The curr... Fig. 7b. X = field data. Solid line = the...

Of the regions of disagreement, t... able occur near the boundary on t... of the geothermal area from the... trodes. In each of the surveys (Figu... the apparent resistivities measured ... are much smaller than those pre... hemispheroidal model. These diff...

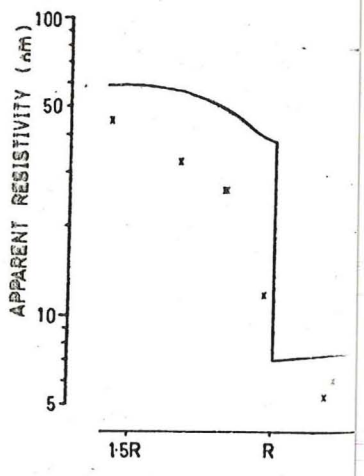

Fig. 10. Curve of theoretical appare... center of the current dipole. The curre... Fig. 8b. X = field data. Solid line = theor...

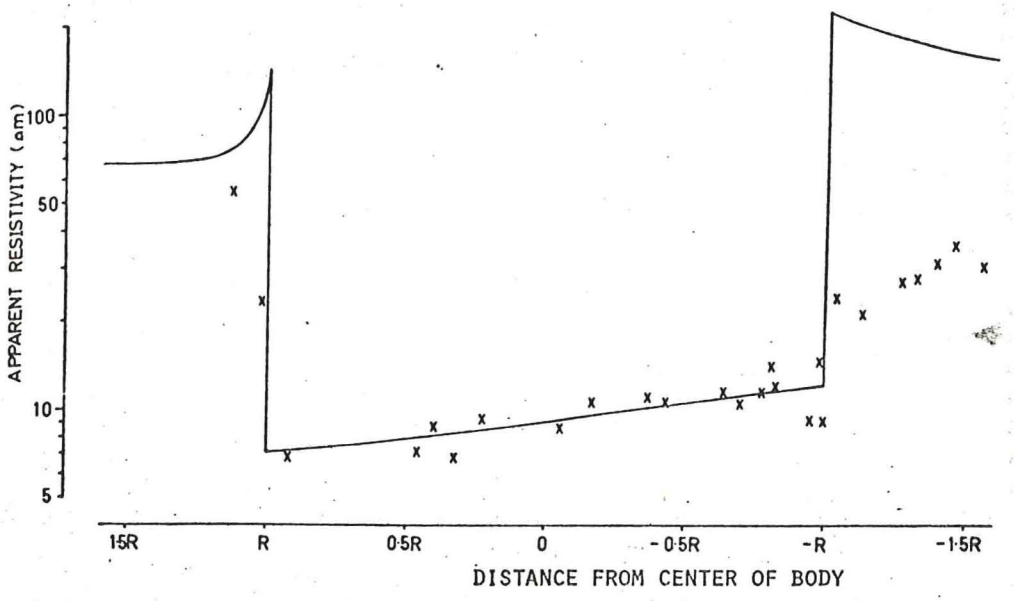

FIG. 9. Curve of theoretical apparent resistivity which best fits the field data along the diameter through the center of the current dipole. The current electrodes lie to the left of the diagram. The case shown corresponds to Fig. 7b. X = field data. Solid line = theoretical profile. ρ'' = 3.35 ohm-m. D/R = 1.02. ρ' = 67 ohm-m.

Of the regions of disagreement, the most noticeable occur near the boundary on the opposite side of the geothermal area from the current electrodes. In each of the surveys (Figures 6, 7, and 8) the apparent resistivities measured in this position are much smaller than those predicted by the hemispheroidal model. These differences, which are clearly shown in Figures 8 and 10, are largest outside the boundary, although, to a lesser extent, they also occur just inside the boundary. This most probably indicates that the geothermal area contains some low-resistivity material in addition to that allowed for by the hemispheroidal model. A possible explanation is that the horizontal

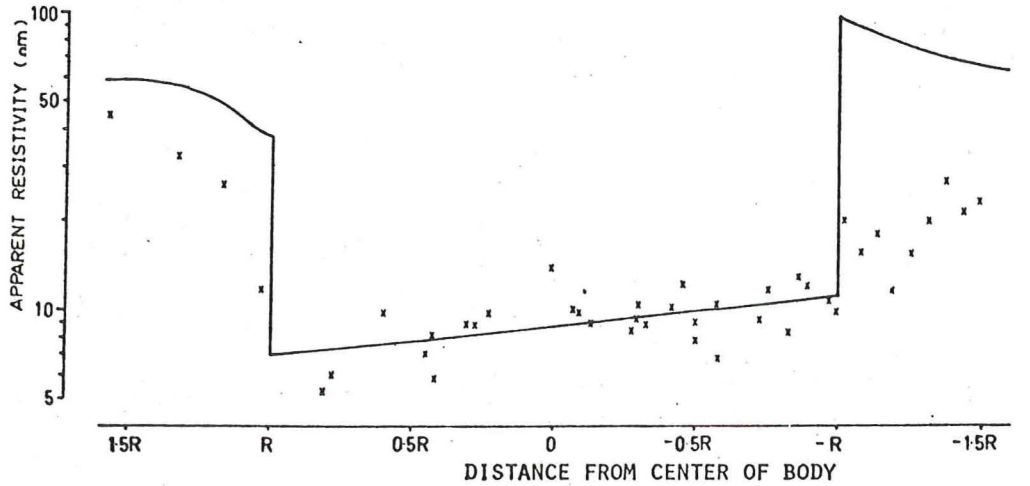

FIG. 10. Curve of theoretical apparent resistivity which best fits the field data along the diameter through the center of the current dipole. The current electrodes lie to the left of the diagram. The case shown corresponds to Fig. 8b. X = field data. Solid line = theoretical profile. ρ'' = 2.95 ohm-m. ρ' = 59 ohm-m. D/R = 0.82.

R, and ρ'/ρ'' by a least-
erse lines through the
des.

itting	Values set
ρ'/ρ"	ρ'/ρ"
44 ± 30	--
--	15
--	20
--	30
16 ± 27	--
--	15
--	20
--	30
35 ± 40	--
--	15
--	20
--	30

eement between the theoretical
istivities. Inside the geothermal
agreement is found, although
areas where significant differ-
e boundary where the theoreti-
ivities have a discontinuity, the
ies increase sharply along most
but along the eastern side a
resistivity is observed rather
ty. Although the shape of the
y circular, a significant irregu-
northeast. Outside the bound-
t is poor, but in some areas
- or low-apparent resistivities
ed, similar highs or lows are

radius of the geothermal reservoir increases near the bottom of the reservoir to a value greater than the surface radius. Alternatively, a low-resistivity layer underlying the geothermal area could be the cause of these differences. The theoretical solution cannot be easily extended to include either of these modifications to the model. Hence, a more accurate estimate of the depth of the geothermal reservoir cannot be obtained. However, qualitative reasoning suggests that the estimate of D obtained in the last section may possibly be too great.

Another area where the observed and theoretical apparent resistivities differ in each of the surveys is the northwest part of the low-resistivity region (Figures 6b, 7b, and 8b). These deviations may be caused by the irregular nature of the boundary in this vicinity. However, a recent detailed resistivity survey of this area has shown that in some places the rocks exhibit pronounced resistivity anisotropy which is thought to be caused by fractures. This suggests that resistivity anisotropy could also be a possible explanation of the deviations.

FURTHER DISCUSSION OF THE THEORETICAL MODEL

In carrying out the kind of survey discussed above, the current electrodes are kept in a fixed position while measurements are made at a large number of receiver array sites. However, the apparent resistivity ρ_a obtained at a particular site is dependent on the resistivity of not only the material beneath that site but also, to different extents, of all the material present. Hence substantial variations of ρ_a can occur in regions where the underlying resistivity is constant. This is clearly shown by the theoretical contours in Figures 6a, 7a, and 8a. Thus, in interpreting dipole-dipole resistivity data, care must be taken not to associate, necessarily, changes of apparent resistivity with changes of the resistivity of the material underlying the receiver sites.

For the case of a hemispheroidal model, the theoretical examples show that ρ_a differs most from the local underlying resistivity for receiver sites just outside the boundary. In extreme cases, ρ_a can be several times larger or smaller than the underlying resistivity. For receiver sites inside the hemispheroid, ρ_a is always greater than the resis-

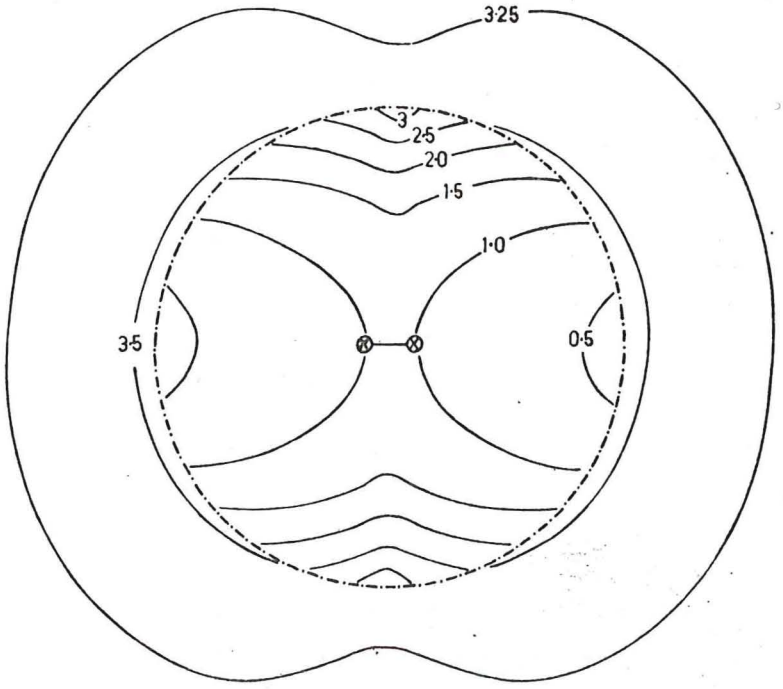

FIG. 11. Contours of the theoretical apparent resistivity ratio ρ_a/ρ'' for current electrodes near the center of a hemispheroid with parameters $\rho'/\rho''=20$, $D/R=0.7$.

tivity of the hemispheroidal ma
in a regular way.

The apparent resistivity con
boundary varies from being e
resistivity contrast when the ele
E is perpendicular to the bound
E is parallel to the boundary. He
problem of locating every point
ary requires that observations be
than one placement of the cur

Difficulties in interpretation c
if the current electrodes are pla
resistivity region. This is illust
oretical apparent-resistivity co
Figure 11. Over more than hal
the apparent-resistivity contra
even though the true-resistivity
Furthermore, outside the hemi
parent resistivities are everyw
fifth of the resistivity of the
Hence for this electrode placem
is scarcely detectable, and use
unlikely to be obtained from t
tivities. This demonstrates tha
hood of misinterpretation by
dipole technique in a region whe
resistivity information is availa

For a hemispheroid of high-re
the converse is true. By placing
trodes inside the hemispheroid,
of apparent resistivity across
obtained, and there is less likel
preting the data. Thus, in both
electrodes should be placed
resistivity material.

CONCLUSION

The interpretation of the dip
of the Broadlands region indica
material of comparatively hig
depth of between 1.3 and 2.7 k
the saturated porous medium
the reservoir of geothermal flu
depth range has been derived fr
at best, an approximation to
cal shape of the reservoir, the a
that there is a region of high r
the reservoir.

Gravity surveys and dri
Hochstein and Hunt, 1970) bo
a greywacke basement in the
at 20 degrees to the west fro

ON OF THE THEORETICAL MODEL

the kind of survey discussed electrodes are kept in a fixed surements are made at a large array sites. However, the ap. obtained at a particular site ne resistivity of not only the nat site but also, to different material present. Hence sub. of ρ_a can occur in regions where sistivity is constant. This is ne theoretical contours in Fig. Thus, in interpreting dipole. ata, care must be taken not to ly, changes of apparent resis- s of the resistivity of the ma- e receiver sites.

a hemispheroidal model, the es show that ρ_a differs most erlying resistivity for receiver e boundary. In extreme cases, mes larger or smaller than the ty. For receiver sites inside the always greater than the resis-

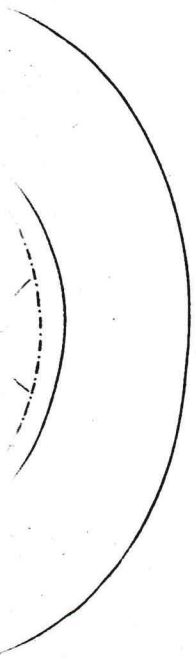

current electrodes near
$/R=0.7$.

vity of the hemispheroidal material and varies a regular way.

The apparent resistivity contrast across the oundary varies from being equal to the true sistivity contrast when the electric field vector E is perpendicular to the boundary, to zero when E is parallel to the boundary. Hence, the practical problem of locating every point on such a boundary requires that observations be made with more than one placement of the current electrodes.

Difficulties in interpretation can be encountered if the current electrodes are placed inside a low-resistivity region. This is illustrated by the theoretical apparent-resistivity contours shown in Figure 11. Over more than half of the boundary the apparent-resistivity contrast is less than 3:1 even though the true-resistivity contrast is 20:1. Furthermore, outside the hemispheroid, the apparent resistivities are everywhere less than a fifth of the resistivity of the exterior material. Hence for this electrode placement the boundary is scarcely detectable, and useful information is unlikely to be obtained from the apparent resistivities. This demonstrates that there is a likelihood of misinterpretation by using the dipole-dipole technique in a region where no independent resistivity information is available.

For a hemispheroid of high-resistivity material the converse is true. By placing the current electrodes inside the hemispheroid, a better contrast of apparent resistivity across the boundary is obtained, and there is less likelihood of misinterpreting the data. Thus, in both cases the current electrodes should be placed within the high-resistivity material.

CONCLUSION

The interpretation of the dipole-dipole surveys of the Broadlands region indicates that there is a material of comparatively high resistivity at a depth of between 1.3 and 2.7 km. Above this lies the saturated porous medium which constitutes the reservoir of geothermal fluids. Although the depth range has been derived from a model which is, at best, an approximation to the actual physical shape of the reservoir, the analysis establishes that there is a region of high resistivity beneath the reservoir.

Gravity surveys and drilling information (Hochstein and Hunt, 1970) both show that there is a greywacke basement in the area which dips at 20 degrees to the west from the Kaingaroa Scarp (see Figure 1) and passes below the geothermal field at depths of between 1.5 and 2.5 km. Measurements of drill cores have shown that the mean porosity of the greywacke is about 5 percent whereas that of the overlying rocks is about 25 percent. Thus, even though comparable temperatures exist throughout the two kinds of rock, the greywacke will have a much higher resistivity than the overlying rocks. This strongly suggests that the high-resistivity material beneath the geothermal reservoir is greywacke. Even though the greywacke contains a smaller proportion of geothermal fluids than the reservoir, the possibility that it may be sufficiently fractured to allow the passage of fluids to the reservoir from greater depths cannot be excluded.

Thus, the depth of the geothermal reservoir is about 2 km, as deduced from the dipole-dipole resistivity field data by using the theoretical method of interpretation developed in this paper, which agrees well with other independent measurements.

ACKNOWLEDGMENT

It is a pleasure to thank Dr. M. P. Hochstein for his helpful criticisms of the manuscript and for his contribution to the development of the ideas it contains.

REFERENCES

Al'pin, L. M., 1966, The theory of dipole soundings, *in* Dipole methods for measuring earth conductivity: New York, Consultants Bureau, p. 1–60.

Anderson, L. A., and Keller, G. V., 1966, Experimental deep resistivity probes in the central and eastern United States: Geophysics, v. 31, p. 1105–1122.

Cook, K. L., and Van Nostrand, R. G., 1954, Interpretation of resistivity data over filled sinks: Geophysics, v. 19, p. 761–770.

Erdélyi, A., 1953, editor, Higher transcendental functions: New York, McGraw-Hill Book Co., Inc.

Fröhlich, R. K., 1968, The influence of lateral inhomogeneities on the dipole methods: Geophys. Prosp., v. 16, p. 314–325.

Hochstein, M. P., and Hunt, T. M., 1970, Seismic gravity and magnetic studies, Broadlands geothermal field, New Zealand: Geothermics, special issue 2, v. 2, p. 333–346.

Keller, G. V., 1966, Dipole methods for deep resistivity studies: Geophysics, v. 31, p. 1088–1104.

Keller, G. V., and Frischknecht, F. C., 1966, Electrical methods in geophysical prospecting: Oxford, Pergamon Press Inc.

Risk, G. F., Macdonald, W. J. P., and Dawson, G. B., 1970, D.C. resistivity surveys of the Broadlands geothermal region, New Zealand: Geothermics, special issue 2, v. 2, p. 287–294.

Seigel, H. O., 1952, Ore body size determination in electrical prospecting: Geophysics, v. 17, p. 907–914.

Zohdy, A. A. R., 1970, Geometric factors of bipole-dipole arrays: Geol. Surv. Bull., 1313-B.

APPENDIX A

FURTHER SOLUTIONS FOR THE POTENTIAL NEAR A HEMISPHEROID

With the notation used in Figure 3 and the accompanying text, the solutions corresponding to equations (2), (3), and (4) are as follows:

1. Electrode A inside the hemispheroid, electrode B outside.

Prolate hemispheroid

$$U(r,\phi,0) = \frac{I}{2\pi}\left\{\left(\frac{\rho'}{R_a}-\frac{\rho''}{R_b}\right)+\frac{(\rho''-\rho')}{(D^2-R^2)^{\frac{1}{2}}}\sum_{n=0}^{\infty}\sum_{m=0}^{n}\frac{(2n+1)(2-\delta_{m0})}{(-1)^m}\times\left[\frac{(n-m)!}{(n+m)!}P_n^m(0)\right]^2\right.$$
$$\left.\times\frac{[\rho' P_n^{m\prime}(\eta_1)Q_n^m(\eta_a)\cos m(\phi-\phi_a)-\rho'' Q_n^{m\prime}(\eta_1)P_n^m(\eta_a)\cos m(\phi-\phi_a)]}{\rho' P_n^{m\prime}(\eta_1)Q_n^m(\eta_1)-\rho'' P_n^m(\eta_1)Q_n^{m\prime}(\eta_1)}\times\begin{Bmatrix}Q_n^m(\eta)P_n^m(\eta_1)\\ P_n^m(\eta)Q_n^m(\eta_1)\end{Bmatrix}\right\}\quad\begin{matrix}\text{for}\\ \\ \end{matrix}\begin{matrix}r>R\\ r<R,\end{matrix}\tag{A1}$$

where

$$\eta=[1+r^2/(D^2-R^2)]^{\frac{1}{2}},\qquad \eta_1=D/(D^2-R^2)^{\frac{1}{2}}.$$

Oblate hemispheroid

$$U(r,\phi,0)=\frac{I}{2\pi}\left\{\left(\frac{\rho'}{R_a}-\frac{\rho''}{R_b}\right)-\frac{i(\rho''-\rho')}{(R^2-D^2)^{\frac{1}{2}}}\sum_{n=0}^{\infty}\sum_{m=0}^{n}\frac{(2n+1)(2-\delta_{m0})}{(-1)^m}\right.$$
$$\times\frac{[\rho' P_n^{m\prime}(i\zeta_1)Q_n^m(i\zeta_a)\cos m(\phi-\phi_a)-\rho'' P_n^m(i\zeta_b)Q_n^{m\prime}(i\zeta_1)\cos m(\phi-\phi_b)]}{\rho' P_n^{m\prime}(i\zeta_1)Q_n^m(i\zeta_1)-\rho'' P_n^m(i\zeta_1)Q_n^m(i\zeta_1)}\times\left[\frac{(n-m)!}{(n+m)!}P_n^m(0)\right]^2\times\left.\begin{Bmatrix}P_n^m(i\zeta_1)Q_n^m(i\zeta)\\ P_n^m(i\zeta)Q_n^m(i\zeta_1)\end{Bmatrix}\right\}\quad\begin{matrix}\text{for}\\ \\ \end{matrix}\begin{matrix}r>R\\ r<R,\end{matrix}\tag{A2}$$

where

$$\zeta=[r^2/(R^2-D^2)-1]^{\frac{1}{2}},\qquad \zeta_1=D/(R^2-D^2)^{\frac{1}{2}}.$$

For small values of r, ζ and ζ_b become imaginary, in which case equation (A2) is still valid provided $P_n^m(i\zeta)$ is replaced by $i^{nm}P_n^m(\mu)$, where $\mu^2=-\zeta^2$.

Hemisphere

$$U(r,\phi,0)=\frac{I}{2\pi}\left\{\left(\frac{\rho'}{R_a}-\frac{\rho''}{R_b}\right)+\frac{\rho''-\rho'}{\rho''+\rho'}\sum_{n=0}^{\infty}\frac{\rho''+\rho'}{\rho''+n(\rho''+\rho')}\right.$$
$$\left.\times\left[n(R/r_a)^{n+1}P_n[\cos(\phi-\phi_a)]+(n+1)(r_b/R)^n P_n[\cos(\phi-\phi_b)]\right]\begin{Bmatrix}R^n r^{-n-1}\\ R^{-n-1}r^n\end{Bmatrix}\right\}\quad\begin{matrix}\text{for}\\ \\ \end{matrix}\begin{matrix}r>R\\ r<R.\end{matrix}\tag{A3}$$

2. Both electrodes inside the

Prolate hemispheroid

$$U(r,\phi,0)=\frac{I\rho''}{2\pi}\left\{\left(\frac{1}{R_a}-\frac{1}{R_b}\right)\times\left[\frac{(n-m)!}{(n+m)!}P_n^m\right.\right.$$
$$\left.\left.\times\begin{Bmatrix}P_n^m(\eta_1)Q_n^m(\eta)\\ P_n^m(\eta)Q_n^m(\eta_1)\end{Bmatrix}\right\}$$

Oblate hemispheroid

$$U(r,\phi,0)=\frac{I\rho''}{2\pi}\left\{\left(\frac{1}{R_a}-\frac{1}{R_b}\right)-\right.$$
$$\times\left[\frac{(n-m)!}{(n+m)!}P_n^m(0)\right.$$
$$\left.\times\begin{Bmatrix}P_n^m(i\zeta_1)Q_n^m(i\zeta)\\ P_n^m(i\zeta)Q_n^m(i\zeta_1)\end{Bmatrix}\right\}\text{ for}$$

Again, when ζ_a, ζ_b, ζ, become ima

Hemisphere

$$U(r,\phi,0)=\frac{I\rho''}{2\pi}\left\{\left(\frac{1}{R_a}-\right.\right.$$
$$\times\frac{1}{R^n}\left[r_a^n P_n[\cos\right.$$

2. Both electrodes inside the hemispheroid.

Prolate hemispheroid

$$U(r,\phi,0) = \frac{I\rho''}{2\pi}\left\{\left(\frac{1}{R_a}-\frac{1}{R_b}\right)+\frac{(\rho''-\rho')}{(D^2-R^2)^{\frac{1}{2}}}\sum_{n=0}^{\infty}\sum_{m=0}^{n}\frac{(2n+1)(2-\delta_{m0})}{(-1)^m}\right.$$
$$\times\left[\frac{(n-m)!}{(n+m)!}P_n^m(0)\right]^2\frac{Q_n^{m\prime}(\eta_1)[P_n^m(\eta_a)\cos m(\phi-\phi_a)-P_n^m(\eta_b)\cos m(\phi-\phi_b)]}{\rho' P_n^{m\prime}(\eta_1)Q_n^m(\eta_1)-\rho'' P_n^m(\eta_1)Q_n^{m\prime}(\eta_1)}$$
$$\left.\times\begin{matrix}P_n^m(\eta_1)Q_n^m(\eta)\\P_n^m(\eta)Q_n^m(\eta_1)\end{matrix}\right\}\quad\text{for}\quad\begin{matrix}r>R\\r<R.\end{matrix}\tag{A4}$$

Oblate hemispheroid

$$U(r,\phi,0) = \frac{I\rho''}{2\pi}\left\{\left(\frac{1}{R_a}-\frac{1}{R_b}\right)-\frac{i(\rho''-\rho')}{(R^2-D^2)^{\frac{1}{2}}}\sum_{n=0}^{\infty}\sum_{m=0}^{n}\frac{(2n+1)(2-\delta_{m0})}{(-1)^m}\right.$$
$$\times\left[\frac{(n-m)!}{(n+m)!}P_n^m(0)\right]^2\frac{Q_n^{m1}(i\zeta_1)[P_n^m(i\zeta_a)\cos m(\phi-\phi_c)-P_n^m(i\zeta_b)\cos m(\phi-\phi_b)]}{\rho' P_n^{m1}(i\zeta_1)Q_n^m(i\zeta_1)-\rho'' P_n^m(i\zeta)Q_n^m(i\zeta_1)}$$
$$\left.\times\begin{matrix}P_n^m(i\zeta_1)Q_n^m(i\zeta)\\P_n^m(i\zeta)Q_n^m(i\zeta_1)\end{matrix}\right\}\text{for}\begin{matrix}r>R\\r<R.\end{matrix}\tag{A5}$$

Again, when ζ_a, ζ_b, ζ, become imaginary, $P_n^m(i\zeta)$ must be replaced by $i^{n+m}P_n^m(\mu)$ where $\mu^2=-\zeta^2$.

Hemisphere

$$U(r,\phi,0) = \frac{I\rho''}{2\pi}\left\{\left(\frac{1}{R_a}-\frac{1}{R_b}\right)-(\rho''-\rho')\sum_{n=0}^{\infty}\frac{(n+1)}{\rho''+n(\rho''+\rho')}\right.$$
$$\left.\times\frac{1}{R^n}\left[r_a^n P_n[\cos(\phi-\phi_a)]-r_b^n P_n[\cos(\phi-\phi_b)]\right]\begin{matrix}R^n r^{-n-1}\\r^n R^{-n-1}\end{matrix}\right\}\text{for}\begin{matrix}r>R\\r<R.\end{matrix}\tag{A6}$$

APPENDIX B

PROCEDURE USED FOR GENERATING LEGENDRE FUNCTIONS

Throughout this paper, the definitions of $P_n^m(z)$ and $Q_n^m(z)$ follow those given by Erdélyi (1953).

Wherever possible, recurrence relations were used for generating the functions $P_n^m(z)/m!$ and $Q_n^m(z)/m!$ for progressively increasing n and m. However, in certain cases the generation process magnified the round-off errors so that an alternative method was required.

For Legendre functions of the first kind, $P_n^m(z)$, the recurrence relations are sufficiently stable to be used in all cases except for z real and less than unity. In this exceptional case the stability was found to be improved by generating $P_n^m(z)/m!$ for decreasing m, starting with $P_n^n(z)/n!$ which can be easily and accurately calculated. This method was checked by calculating $P_n^0(z)$ from the hypergeometric function.

The Legendre functions of the second kind are not sufficiently stable under generation by recurrence relations for increasing n. This difficulty was overcome by generating $Q_n^0(z)$ from hypergeometric functions using the following expressions:

$$Q_n^0(z) = \pi^{\frac{1}{2}} n! F(1+n/2, 0.5+n/2;\ n+1.5;\ z^{-2}) / (2z)^{n+1}\Gamma(n+1.5) \quad \text{(B1)}$$

for z real and greater than unity,
and

$$Q_n^0(z) = \pi^{\frac{1}{2}} n!(z^2-1)^{-\frac{1}{4}}[z-(z^2-1)^{\frac{1}{2}}]^{n+\frac{1}{2}} \cdot F(0.5, 0.5;\ n+1.5;\ 0.5-0.5z \quad \text{(B2)}$$
$$/(z^2-1)^{\frac{1}{2}})/\Gamma(n+1.5)$$

for pure imaginary z, where $F(a, b;\ c;\ \zeta)$ is the hypergeometric function in ζ. Recurrence relations can then be used to generate $Q_n^m(z)$ for increasing values of m.

A COMPARISON OF IP E

J. H. COGGON*

The responses of dipole-dipole, pc
radient arrays to a set of ten st
been computed using the finite ele
Comparison of the responses indic
The dipole-dipole array usually giv
anomalies, but the anomalies rarel
tion on dip of a structure and are
enced by overburden irregularitie
gives best overall resolution.
anomalies are almost as large as
ones and have the same general
less resolution. The lower resolu
asymmetry of this array make
difficult to interpret. (3) The grad
vides dip information and good hor
tion. Responses to thin vertical
weak, anomalies are strongly affe
burden irregularities, and there
depth discrimination.

ARRAYS

A variety of electrode arrays is
exploration with the induced-polari
The choice of array should be guic
pose of a survey, the geologic situ
amount of information desired.
there is some tendency for the use
array to become routine and for in
sideration to be given to the ch
different arrays. Indeed, there is
actual information on the advanta
tions of the arrays. However, suc
may be derived from a study of the
alies. In order to compare three co
dipole-dipole, pole-dipole, and gr
discuss their responses to a set o
tures.

The layout of each array is show

* Manuscript received by the Editor A
* University of Otago, Dunedin, New Z
© 1973 Society of Exploration Geophy